ACS APPLIED MATERIALS & INTERFACES
Research Article
www.acsami.org

Manipulated Transformation of Filamentary and Homogeneous Resistive Switching on ZnO Thin Film Memristor with Controllable Multistate

Chi-Hsin Huang,[†,§] Jian-Shiou Huang,[†,§] Chih-Chung Lai,[†] Hsin-Wei Huang,[†] Su-Jien Lin,[†] and Yu-Lun Chueh*,[†]

[†]Department of Materials Science and Engineering, Center For Nanotechnology, Material Science, and Microsystem, National Tsing Hua University, Hsinchu, Taiwan, Republic of China

Supporting Information

ABSTRACT: A bias polarity-manipulated transformation from filamentary to homogeneous resistive switching was demonstrated on a Pt/ZnO thin film/Pt device. Two types of switching behaviors, exhibiting different resistive switching characteristics and memory performances were investigated in detail. The detailed transformation mechanisms are systematically proposed. By controlling different compliance currents and RESET-stop voltages, controllable multistate resistances in low resistance states and a high resistance states in the ZnO thin film metal−insulator−metal structure under the homogeneous resistive switching were demonstrated. We believe that findings would open up opportunities to explore the resistive switching mechanisms and performance memristor with multistate storage.

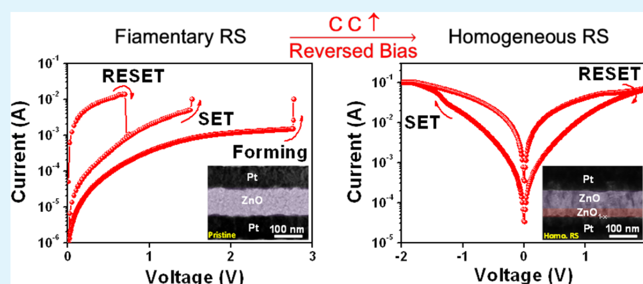

KEYWORDS: *resistive switching, ReRAM, ZnO, memristor, nonvolatile memory, multistate storage*

1. INTRODUCTION

Resistive switching random access memory (ReRAM), consisting of the simplest device configuration, namely metal−insulator−metal (MIM), is the most promising candidate as next generation nonvolatile memory. It has a higher potential to replace current flash memory and dynamic random access memory (DRAM) due to its faster switching speed, higher stacking density, lower power consumption, higher scalability, faster fabrication process, and stronger potential for fabricating multistate memories.[1−3] After intensively investigating the switching mechanisms of ReRAM in recent years, the migration of oxygen vacancies (or oxygen ions) under an applied electrical field plays an important role in the metal oxide materials, for which the resistive switching behaviors are highly determined by the accumulation of oxygen vacancies (or oxygen ions) either at the interface or in the bulk of materials.[1−4]

Typically, two types of resistive switching mechanisms have been proposed, namely, filamentary and homogeneous switching behaviors. The filamentary resistive switching, which is described as fuse−antifuse switching, basically involves the formation and rupture of conducting filaments by thermochemical reactions inside the insulating metal oxide layer.[3] The electrochemical metallization mechanism (ECM) *via* formation of metallic filaments by the accumulation of active metal electrodes, such as Ag and Cu in the electrochemical dissolution, is another case for filamentary switching.[3,5] In addition to filamentary resistive switching, homogeneous interface resistive switching, behaving as continuous switching, is attributed to an asymmetric balance of Schottky-barrier heights induced by the electric field *via* trapping and detrapping processes of carriers through defective states at interfaces between the functional material and electrode.[6,7] The switching current *via* homogeneous switching highly depends on the device area, which guarantees a sufficient current to maintain reliable operation. However, switching current localized by one or several conducting filaments, namely filamentary resistive switching, may result in the fluctuation of resistance states and a larger current density, thus unstable operation in the scaled device once the area of the device becomes smaller.

Some materials, such as WO_x,[8] Fe-doped $SrTiO_3$,[9,10] and $DyMn_2O_5$,[11] have been found that the coexistence of filamentary and homogeneous resistive switching has been illustrated, while how to control the transformation between filamentary and homogeneous resistive switching has not been reported yet. In addition, the transition from bipolar to unipolar resistive switching relying on current compliance by an electroforming process has been observed in TiO_2,[12] while filamentary and homogeneous resistive switching exhibiting different switching characteristics and device performances have

Received: February 26, 2013
Accepted: May 24, 2013
Published: May 24, 2013

 © 2013 American Chemical Society

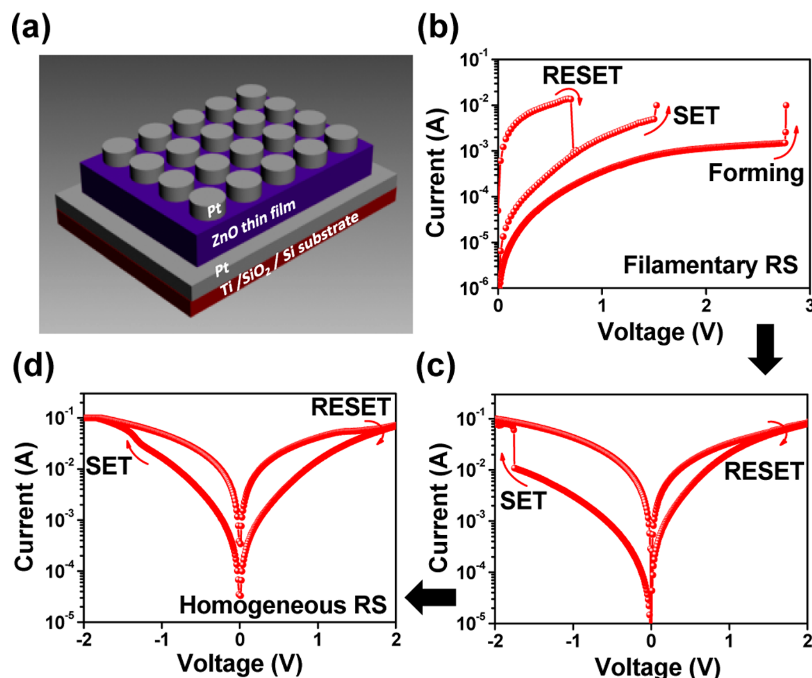

Figure 1. (a) Schematic of a Pt/ZnO thin film/Pt resistive switching device. (b) *I*−*V* characteristics of a filamentary resistive switching for the Pt/ZnO/Pt devices. (c) *I*−*V* characteristics of the transformation process. (d) *I*−*V* characteristics of the homogeneous resistive switching for the Pt/ZnO thin film/Pt devices.

not yet been investigated systematically. Therefore, it is important to investigate the relationship of two switching mechanisms and the feasibility of controlling the transformation between filamentary and homogeneous resistive switching for further development of ReRAM.

In this regard, we demonstrate a controllable transformation of filamentary to homogeneous interface resistive switching in a ZnO thin film MIM structure *via* different bias polarities. These two types of resistive switching behaviors, which exhibit different resistive switching characteristics and memory performances, were investigated in detail. The possible transformation mechanisms are systematically proposed by microstructural and chemical analyses obtained from transmission electron microscopy (TEM). By controlling different compliance currents (CC) and RESET-stop voltages, we are able to demonstrate a controllable multilevel storage at a high resistance state (HRS) and a low resistance state (LRS) in the ZnO thin film MIM structure under homogeneous resistive switching for high density with multistorage application.

2. EXPERIMENTAL SECTION

Materials and Methods. A 100-nm-thick ZnO thin film was deposited on a Pt/Ti/SiO_2/Si substrate at room temperature by radio frequency (rf) magnetron sputtering using a ceramic ZnO target. The 100-nm-thick Pt top electrode was deposited on the ZnO thin film patterned by a shadow mask *via* rf-magnetron sputtering at room temperature. The diameters of the top electrodes from 200 to 50 μm were also defined by metal shadow masks.

Characterization. Field-emission transmission electron microscopy (JEM-3000F, JEOL operated at 300 kV with a point-to-point resolution of 0.17 nm) equipped with an energy dispersion spectrometer (EDS) was used to obtain the microstructures and the chemical compositions. The crystallinity of the ZnO film was confirmed by X-ray diffraction (Shimadzu XRD 6000, Cu Kα radiation with a wavelength of 0.154 nm). The electrical characterizations and resistive switching characteristics were measured using a Keithley 4200 semiconductor parameter analyzer in voltage sweeping mode at room temperature. All of the operation voltages were applied on the Pt top electrode, with which the Pt bottom electrode was grounded.

3. RESULTS AND DISCUSSION

Figure 1a shows a schematic of the ZnO thin film MIM structure, for which the stacking sequences of the entire structure are Pt (100 nm)/ZnO (100 nm)/Pt (100 nm). The X-ray spectrum confirms a wurtzite structure of the ZnO thin film with a good crystallinity, for which a single peak at the (002) plane could be obviously observed (Figure S1). By applying a positive bias from 0 V to ∼2.8 V (forming voltage) with a compliance current of 10 mA, an abrupt increase of current could be observed, namely the "forming process," for which the resistance of the device is changed from the initial resistance state to LRS owing to the formation of conducting filaments in the ZnO thin film as shown in Figure 1b. When we sweep the biases from 0 V to ∼0.7 V (RESET voltage, V_{RESET}), the resistance of the device changing to HRS was observed, which is called the "RESET process" (Figure 1b). A change of resistance from HRS to LRS, namely the "SET process," could be achieved after a positive bias > 1.5 V (SET voltage, V_{SET}) was applied (Figure 1b). The resistive switching in the ZnO film is called unipolar switching, which is a kind of filamentary resistive switching. To trigger the transformation of filamentary to homogeneous resistive switching, a reverse sweep bias of ∼−1.75 V with a relatively high CC (∼ 100 mA) was applied, with which an abrupt current change from HRS to LRS could be found as shown in Figure 1c. Note that due to the higher CC, a higher current/lower LRS could be observed, as shown in Figure 1c. Subsequently, the bias sweep at a positive bias was applied from 0 V to ∼2 V to conduct the RESET behavior, resulting in the device in the HRS. Finally, SET and RESET biases were applied from 0 to −2 V and 0 to 2 V with a CC of 100 mA, respectively, for which the transformation of the filamentary to the homogeneous switching is accomplished, as

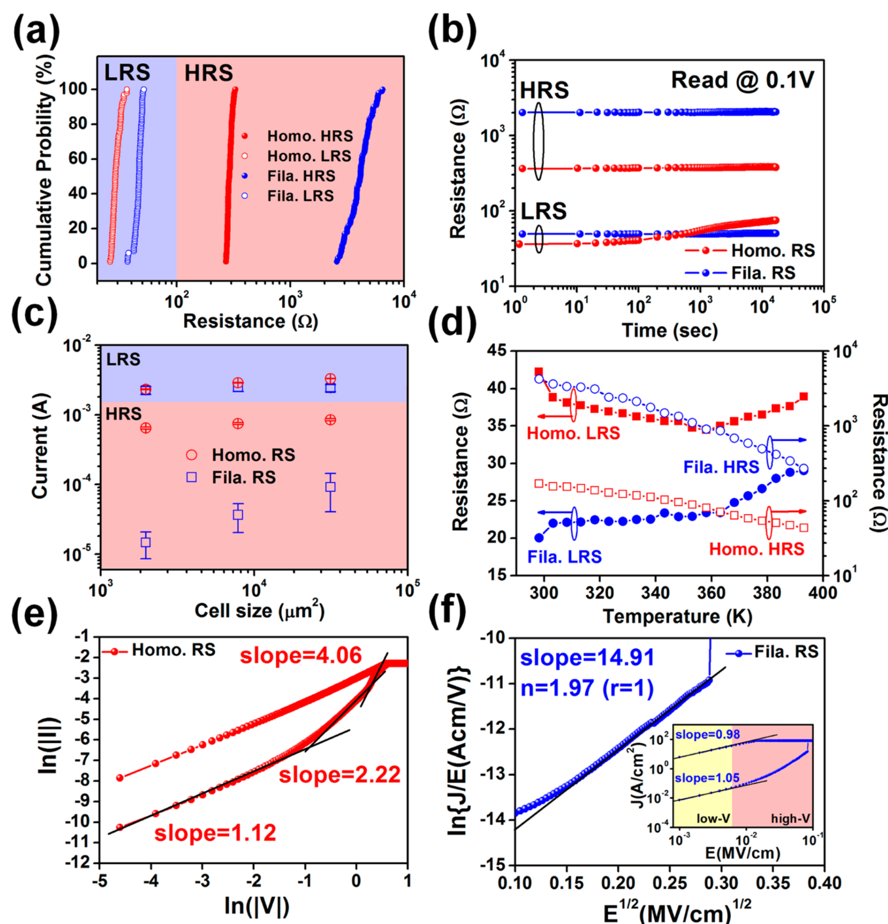

Figure 2. (a) Cumulative distribution of the HRS/LRS for the Pt/ZnO/Pt devices. (b) Retention tests of the filamentary and homogeneous resistive switching under a continuous read voltage of 0.1 V. (c) Currents as the function of device sizes at HRS/LRS of the filamentary and homogeneous resistive switching. The error bar at each cell size is calculated by the standard deviation of 20 devices. (d) Temperature dependences at HRS/LRS for filamentary and homogeneous resistive switching. (e) ln (I)−ln (V) plots for homogeneous resistive switching. (f) ln (J/E) − $E^{1/2}$ and inset J−E plots for filamentary resistive switching.

shown in Figure 1d. In addition, an opposite operation can be obtained if we switch the bias polarity, confirming the stable and controllable process, as shown in Figure S2.

The different resistive switching modes ("fuse−antifuse switching by conducting filaments" versus "continuous switching by trapping−detrapping behaviors *via* the migration of defects/ions")[2,3] for both switching behaviors could be achieved. The fuse−antifuse switching is a typical feature of filamentary switching, which usually manifests in the so-called unipolar resistive switching mode, for which the switching of LRS and HRS occurs owing to the formation and rupture of local metallic paths by Joule heating at the same bias polarity while it can be also operated at any polarity, namely a nonpolar resistive switching mode.[3] In contrast, homogeneous resistive switching involves continuous switching by the trapping−detrapping effect *via* intrinsic defects at the metal/insulator interface or the migrated ions/defects to the interface induced by the electrical field, belonging to bipolar switching.[6,7] Notably, the abrupt current increases in the SET process and sudden decreases in the RESET process are a particular feature of filamentary resistive switching (Figure 1b). After the transformation from filamentary to homogeneous resistive switching, a gradually continuous increase and decrease in current from the current−voltage (I−V) curve could be found during the SET and RESET processes (Figure 1d). In addition, a memristive effect, namely different hysteresis loops due to changes of Schottky-barrier depletion width *via* the charge accumulation and trapping/detrapping processes could be obviously obtained by different positive/negative biases and sweep cycles as shown in Figure S3, evidently indicating the replacement of the filamentary resistive switching by homogeneous resistive switching.[13]

Figure 2a shows cumulative probability distributions of resistances at HRS/LRS by filamentary and homogeneous resistive switching. The corresponding cumulative probability distributions of resistances at V_{SET}/V_{RESET} voltages are shown in Figure S3. The statistic distributions of the resistances (HRS and LRS) and switching threshold voltages (V_{SET} and V_{RESET}) of 100 cycles in the homogeneous resistive switching are nearly vertical with a slight fluctuation, confirming that the switching behavior of homogeneous resistive switching is very uniform. The nonuniform performances for filamentary resistive switching mainly result from variable locations, orientations, and sizes of conducting filaments during SET and RESET processes. The retention test was conducted as shown in Figure 2b to evaluate an ability of nonvolatile data storage. Notably, filamentary resistive switching shows good retention characteristics up to 10^4 s without any degradation in both HRS and LRS. The electrical mechanisms involving the trapping and detrapping of carriers within the interface states for homogeneous switching

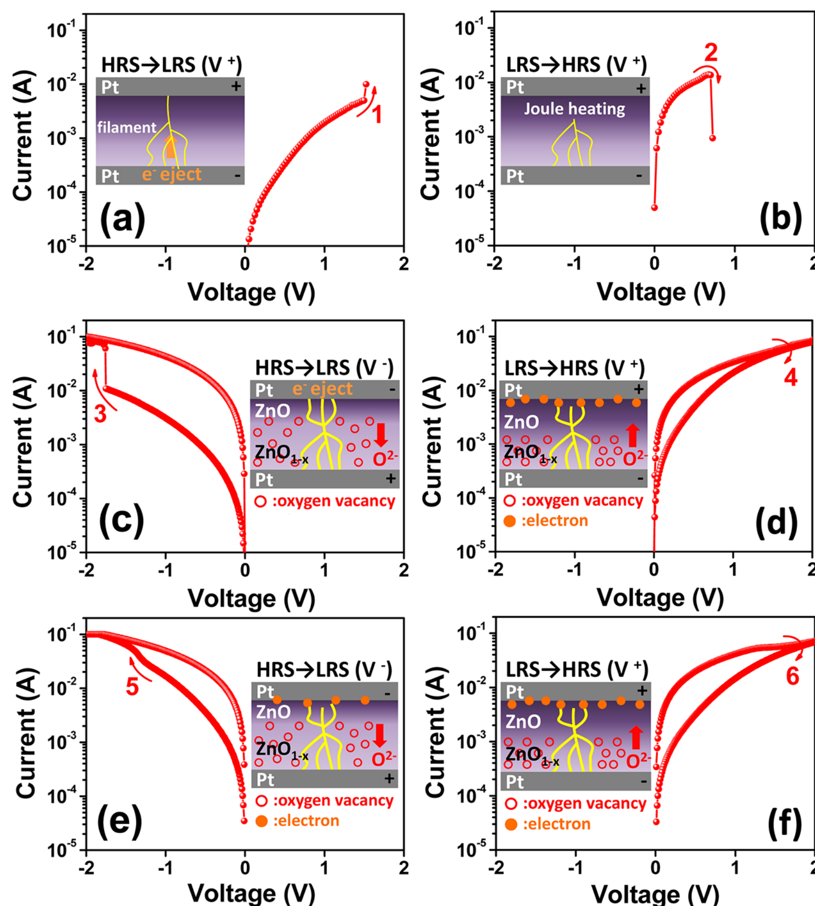

Figure 3. Schematics of transformation mechanisms of filamentary into homogeneous resistive switching.

face a problem of intrinsically low retention time.[14,15] However, the homogeneous resistive switching still maintains a reasonable retention characteristic of $\sim 10^3$ s in our device. To shed light on filamentary and homogeneous resistive switching, the current at HRS and LRS with different electrode sizes was measured, as shown in Figure 2c. Current at HRS and LRS in the homogeneous resistive switching increases as electrode sizes increase, namely slightly linear dependence, indicating that the current is homogeneous throughout the device and the switching occurs on the entire thin film. Notice that the lesser decrease of current trend as the device area decreases is probably due to a lesser resistivity (ρ) modulation at the bigger cell size during the homogeneous operation. The smaller electrodes contain higher resistivity due to a lesser amount of grain boundaries and leakage current. Moreover, the polarity-dependent migration *via* oxygen vacancies induces oxygen-deficient/oxygen-rich region modulation, resulting in different resistivities. However, the current at the HRS in filamentary resistive switching is still dependent on the device sizes while the current at the LRS was found to be independent of the device sizes resulting from the formation of localized conducting filaments.[2] Figure 2d shows temperature dependence studies at changes of resistances from HRS and LRS in filamentary and homogeneous resistive switching. The resistances at HRS in both types decrease with an increase in temperature, which originates from an intrinsic behavior of the ZnO thin film, indicating a semiconducting feature. Interestingly, the resistance at LRS increases with an increase in temperature, indicating a metallic characteristic of filamentary resistive switching while the resistance at LRS in homogeneous resistive switching exhibits an opposite trend, namely a decrease of resistance with an increase of temperature, again confirming the semiconducting behavior. An increase of the resistance at LRS in the homogeneous resistive switching beyond 360 K is most likely from the metallic filaments embedded in the semiconducting ZnO film during the initial unipolar operation. It is because such behavior could be related to either the diffusion of oxygen vacancies in a thin film or the trapped electronic charges at the metal/semiconductor interface or both of them. Figure 2e shows the double-logarithmic plots of the I–V curves for negative voltage regions of homogeneous resistive switching. The log I–V plot at HRS shows an Ohmic conduction behavior, namely a linear proportion for current to voltage at a low voltage region (<2.5 V) gradually changes to the Child's law region, for which the current is proportional to the square of the voltage.[16] This behavior is qualitatively interpreted to follow the shallow trap-associated SCLC theory with a simple equation of $I(V) = aV + bV^2$.[16] The trap-controlled SCLC describes the charge conduction *via* charge trapping and detrapping, which is consistent with previous reports on the Schottky effect, where the migration of oxygen vacancies in the vicinity of the interface drives resistive switching. Under a positive electric field, oxygen vacancies migrate away from the Schottky interface between ZnO and Pt, which changes the Schottky-barrier widths and widens the depletion layer, resulting in HRS and *vice versa*. On the other hand, Poole–Frenkel emission was found to follow typical I–V curves of the filamentary resistive switching in the HRS.[17] A

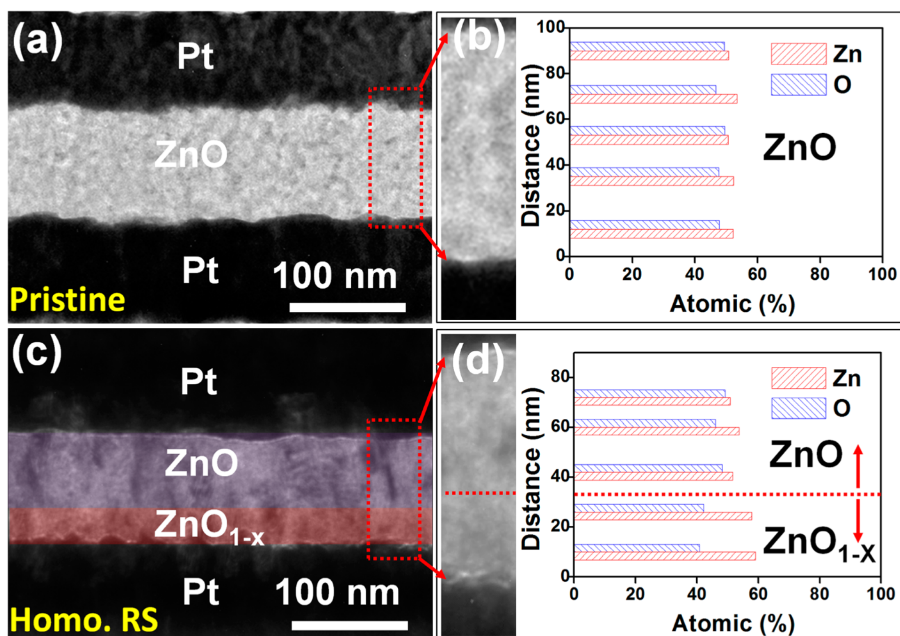

Figure 4. (a) A TEM image of the pristine device. (b) The corresponding EDS elemental profiles. (c) A TEM image of the device after transformation of filamentary into homogeneous resistive switching. (d) The corresponding EDS elemental profiles.

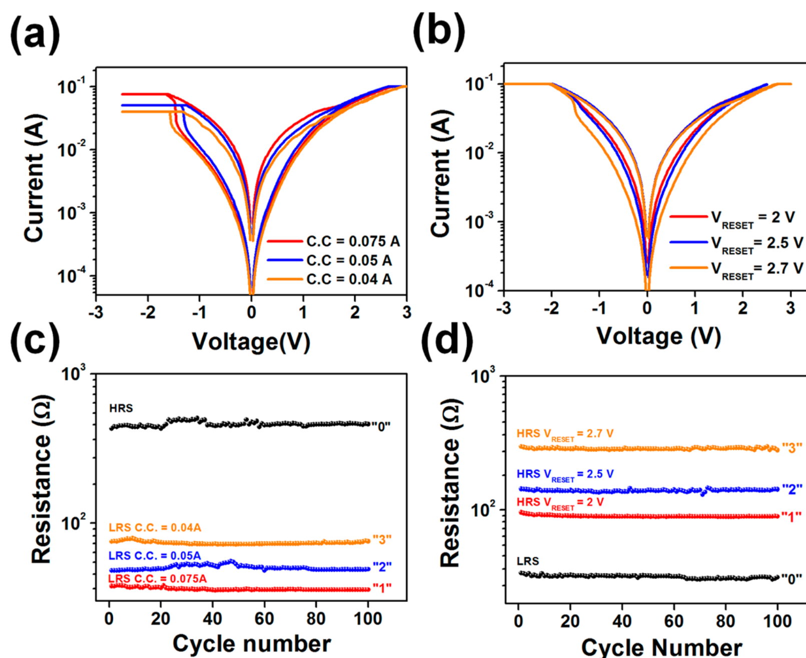

Figure 5. (a) $I-V$ characteristics of homogeneous resistive switching when varying the compliance currents (CC). (b) Endurance tests of 100 cycles for the homogeneous resistive switching when varying the CC at a read bias of 0.1 V. (c) $I-V$ characteristics of the homogeneous resistive switching when varying the RESET-stop voltage. (d) Endurance tests of 100 cycles for the homogeneous resistive switching when varying the RESET-stop voltage at a read bias of 0.1 V.

linear curve with a slope of ~1 was observed in the LRS, which suggests Ohmic conduction, indicating the existence of conducting filaments as shown in inset of Figure 2f. (More detailed modeling of transport mechanisms from the fitting of $I-V$ curves is discussed in the Supporting Information file.)

Therefore, detailed mechanisms on how the transformation of filamentary to homogeneous resistive switching behaviors with controllable biases and polarities were proposed as shown in Figure 3a–f. By applying a large voltage, namely the forming process, the oxygen vacancies are migrated and gathered together to generate conducting filaments located inside the ZnO film to result in the device from HRS to LRS (Figure 3a).[18] Subsequently, the rupture of filaments *via* Joule heating due to the high current density occurred, turning the device from LRS to HRS in the RESET process (Figure 3b).[18,19] Notice that the positions for the rupture of the filaments would normally occur near the top electrode because of much finer filament sizes.[19] When we sweep a large enough negative bias at the top electrode, an abrupt change in current from HRS to LRS could be observed owing to the formation of filament

paths near the top electrode caused by the migration of oxygen vacancies while the compensation of filament paths near the bottom electrode caused by the migration of oxygen ions can be achieved, resulting in the formation of the ZnO_{1-x} (ZnO layer with oxygen-deficient region) layer as shown in Figure 3c. A transition of filamentary to homogeneous resistive switching can be triggered at this stage but is not completed yet until a further positive bias is applied to finish the homogeneous switching. When the positive bias was applied on the top electrode, the O^{2-} would be attracted toward the top electrode from the ZnO_{1-x} layer, resulting in the formation of an oxygen-rich (ZnO) layer near the top electrode, leading to HRS. Consequently, the transformation of the filamentary to the homogeneous resistance switching could be completed (Figure 3d). The following device switching from HRS to LRS is caused by trapping and detrapping processes owing to the asymmetric Schottky-barrier height resulting from stoichiometric modulation of the oxygen-rich layer (e.g., oxygen ion/vacancy electromigration in Figure 3e and f).

To corroborate the existence of the oxygen-defective region nearby the bottom Pt electrode, the energy dispersive spectrum (EDS) was used to obtain the compositional difference in two kinds of samples, namely a pristine sample without any operation and a sample after the transformation of filamentary to homogeneous resistive switching, as shown in Figure 4a and b, respectively. The uniform atomic concentrations of ∼51 atom % Zn and ∼49 atom % O through the entire ZnO thin film for the pristine sample could be observed (Figures 4a) while a Zn rich region (∼25−30-nm-thick), namely the oxygen-defective region with atomic concentrations of ∼60 atom % Zn and ∼40 atom % O could be detected (Figure 4b), distinctly confirming the existence of the oxygen-deficient regions nearby the bottom Pt electrode.

Furthermore, by controlling the different compliance currents (CC) and RESET-stop voltages, we are able to enlarge or deplete the oxygen-defective region, leading to the multistate resistances at LRS and HRS under homogeneous resistive switching, respectively. Figure 5a shows the *I*−*V* characteristics of SET processes after a constant SET bias of −3 V was applied with different CCs of 0.04, 0.05, and 0.075 A, respectively, with which a RESET bias of 3 V was applied for each measurement. It could be clearly seen that varying the compliance currents could result in different resistances at LRS. The higher the CC that was applied, the smaller the resistance at LRS that was obtained, while the resistances at HRS are almost identical (Figure S5a). An endurance test of ∼100 cycles as shown in Figure 5b indicates that resistive switching for each memory state is very stable. On the other hand, by controlling the RESET-stop voltages of 2, 2.5, and 2.7 V, the *I*−*V* characteristics with different resistances at HRS could be achieved as shown in Figure 5c, for which a constant SET voltage of 3 V with a CC of 10 mA was applied for each measurement. Again, the higher resistance at HRS was achieved as the larger RESET-stop voltage was applied (Figure S5b). We found that resistive switching is also very stable at each memory state with an endurance test of ∼100 cycles as shown in Figure 5d. Most importantly, all resistances at HRS and LRS are reversible, depending on the different CC and RESET-stop voltages.

4. CONCLUSIONS

We present a method for the transformation of the filamentary resistive switching into the homogeneous resistive switching for the Pt/ZnO thin films/Pt MIM structure memory device. We believe the critical role of the transformation between filamentary and homogeneous resistive switching highly relies on the distribution of oxygen vacancies. Detailed transformation mechanisms are systematically proposed. By controlling different compliance currents and RESET-stop voltages, we are able to demonstrate controllable multistate resistances at LRS and HRS in the ZnO thin film MIM structure under homogeneous resistive switching. Our method could open up an opportunity to explore not only the resistive switch mechanism but also develop next generation multistate high performance memory.

■ ASSOCIATED CONTENT

Ⓢ Supporting Information

XRD spectrum of ZnO film; *I*−*V* characteristics of the memristive effects; transformation of filamentary to homogeneous switching under an opposite operation; transport mechanism for filamentary and homogeneous resistive switching; demonstration of multistate resistances at LRS and HRS under homogeneous resistive switching. These materials are available free of charge via the Internet http://pubs.acs.org

■ AUTHOR INFORMATION

Corresponding Author

*E-mail: ylchueh@mx.nthu.edu.tw.

Author Contributions

§These two authors contributed equally to this work.

Notes

The authors declare no competing financial interest.

■ ACKNOWLEDGMENTS

The research was supported by the National Science Council through grant nos. NSC 101-2112-M-007-015-MY3 and NSC 100-2120-M-007-008 and National Tsing Hua University through grant no. 102N2022E1. Y.L.C. greatly appreciates the use of the facility at CNMM, the National Tsing Hua University through grant no. 101N2744E1.

■ REFERENCES

(1) Waser, R.; Aono, M. *Nat. Mater.* **2007**, *6*, 833−840.

(2) Sawa, A. *Mater. Today* **2008**, *11*, 28−36.

(3) Waser, R.; Dittmann, R.; Staikov, G.; Szot, K. *Adv. Mater.* **2009**, *21*, 2632−2663.

(4) Huang, C. H.; Huang, J. S.; Lin, S. M.; Chang, W. Y.; He, J. H.; Chueh, Y. L. *ACS Nano* **2012**, *6*, 8407−8414.

(5) Yang, Y. C.; Pan, F.; Liu, Q.; Liu, M.; Zeng, F. *Nano Lett.* **2009**, *9*, 1636−1643.

(6) Sawa, A.; Fujii, T.; Kawasaki, M.; Tokura, Y. *Appl. Phys. Lett.* **2004**, *85*, 4073−4075.

(7) Yang, J. J.; Pickett, M. D.; Li, X.; Ohlberg, D. A. A.; Stewart, D. R.; Williams, R. S. *Nat. Nanotechnol.* **2008**, *3*, 429−433.

(8) Biju, K. P.; Liu, X.; Kim, S.; Jung, S.; Park, J.; Hwang, H. *Phys. Status Solidi RRL* **2011**, *5*, 89−91.

(9) Shibuya, K.; Dittmann, R.; Mi, S.; Waser, R. *Adv. Mater.* **2010**, *22*, 411−414.

(10) Muenstermann, R.; Menke, T.; Dittmann, R.; Waser, R. *Adv. Mater.* **2010**, *22*, 4819−4822.

(11) Tsai, Y. T.; Chang, T. C.; Huang, W. L.; Huang, C. W.; Syu, Y. E.; Chen, S. C.; Sze, S. M.; Tsai, M. J.; Tseng, T. Y. *Appl. Phys. Lett.* **2011**, *99*, 092106−3.

(12) Jeong, D. S.; Schroeder, H.; Waser, R. *Electrochem. Solid-State Lett.* **2007**, *10*, G51−G53.

(13) Strukov, D. B.; Snider, G. S.; Stewart, D. R.; Williams, R. S. *Nature* **2008**, *453*, 80−83.
(14) Peng, H. Y.; Li, G. P.; Ye, J. Y.; Wei, Z. P.; Zhang, Z.; Wang, D. D.; Xing, G. Z.; Wu, T. *Appl. Phys. Lett.* **2010**, *96*, 192113−3.
(15) Schroeder, H.; Zhirnov, V. V.; Cavin, R. K.; Waser, R. *J. Appl. Phys.* **2010**, *107*, 054517−8.
(16) Lampert, M. A. *Phys. Rev.* **1956**, *103*, 1648−1656.
(17) Yeargan, J. R.; Taylor, H. L. *J. Appl. Phys.* **1968**, *39*, 5600−5604.
(18) Kim, M. K.; Jeong, D. S..; Hwang, C. S. *Nanotechnol.* **2011**, *22*, 254002−17.
(19) Chang, S. H.; Lee, J. S.; Chae, S. C.; Lee, S. B.; Liu, C.; Kahng, B.; Kim, D. W.; Noh, T. W. *Phys. Rev. Lett.* **2009**, *102*, 026801−4.